

PPAR α deficiency exacerbates retinal pathological changes and dysfunction in high-fat diet mice

Xue Wang^{1,2,3}, Jing-Jing Ding^{1,4}, Chao-Feng Yu³, Deng-Cheng Xiao^{1,4}, Li-Ming Tao¹, Zheng-Xuan Jiang¹

¹Department of Ophthalmology, the Second Affiliated Hospital of Anhui Medical University, Anhui Medical University, Hefei 230000, Anhui Province, China

²University of Science and Technology of China, Suzhou Institute of Biomedical Engineering and Technology, Suzhou 215163, Jiangsu Province, China

³Aier Academy of Ophthalmology, Central South University, Changsha 410018, Hunan Province, China

⁴Department of Clinical Medicine, the Second School of Clinical Medicine, Anhui Medical University, Hefei 230022, Anhui Province, China

Correspondence to: Li-Ming Tao and Zheng-Xuan Jiang, Department of Ophthalmology, the Second Affiliated Hospital of Anhui Medical University, Anhui Medical University, Hefei 230000, Anhui Province, China. lmtao@163.com; jiangzhengxuan@ahmu.edu.cn

Received: 2024-10-25 Accepted: 2025-03-05

Abstract

• **AIM:** To examine the effects of a high-fat diet (HFD) on retinal pathological changes and dysfunction using peroxisome proliferator-activated receptor-alpha (PPAR α) knockout mice.

• **METHODS:** For four months, C57BL/6J and PPAR α knockout mice received either HFD or a standard diet (SD). A fluorometric method was used to determine the retinal triglycerides. The retinal malondialdehyde (MDA) content was measured. Hematoxylin-eosin was used to evaluate retinal pathological changes. Protein expression was analyzed by Western blot and immunofluorescence, while mRNA expression was evaluated by quantitative reverse transcription-polymerase chain reaction. Electroretinogram was used to assess retinal function.

• **RESULTS:** HFD resulted in increased fatty acid β -oxidation in the inner retina, particularly retinal ganglion cells (RGCs), as well as increased weight and accumulation of retinal triglyceride. Retinal fatty acid β -oxidation and triglyceride accumulation were affected by PPAR α ^{-/-} abnormalities. PPAR α knockdown increased the infiltration and activation of inflammatory cells, as well as

it upregulated the nuclear factor kappa B (NF- κ B) signaling pathway and corresponding proinflammatory cytokine levels in the most retina subjected to the HFD. In the HFD mice, oxidative stress levels were elevated in the inner retina, particularly in the HFD PPAR α ^{-/-} mice. HFD-induced RGCs apoptosis initiation was exacerbated by PPAR α deficiency. Lastly, HFD feeding resulted in the lower amplitudes of scotopic a-wave, b-wave and photopic negative response (PhNR) wave, particularly in HFD PPAR α ^{-/-} mice.

• **CONCLUSION:** In HFD-fed mice retina, particularly in the inner retina, PPAR α knockout increases lipid metabolic abnormalities, inflammatory responses, oxidative stress, apoptosis initiation and dysfunction.

• **KEYWORDS:** peroxisome proliferator-activated receptor-alpha; high-fat diet; retina; electroretinogram

DOI:10.18240/ijo.2025.06.03

Citation: Wang X, Ding JJ, Yu CF, Xiao DC, Tao LM, Jiang ZX. PPAR α deficiency exacerbates retinal pathological changes and dysfunction in high-fat diet mice. *Int J Ophthalmol* 2025;18(6):986-995

INTRODUCTION

Nervous system disorders, metabolic syndrome and type 2 diabetic mellitus have been investigated using high-fat diet (HFD) animals^[1-3]. In Alzheimer's and Parkinson's models, HFD exacerbated central nervous degeneration^[4-5]. The metabolic disorder brought on by HFD, was a significant risk factor for diabetic retinopathy and retinitis pigmentosa^[1,6]. In HFD-induced diabetes model, retinal neurodegeneration, especially retinal ganglion cells (RGCs) synaptic loss, preceded retinal microvascular pathological changes^[1]. In retinitis pigmentosa model, short-term HFD feeding exacerbated photoreceptor degeneration and microglial cell activation, besides, triggered the inflammation-related pathway and oxidative stress in retina^[6]. However, the direct role of lipid metabolism in HFD-induced retinal degeneration remained unclear.

A ligand-activated transcription factor named the peroxisome proliferator-activated receptor-alpha (PPAR α) plays a significant role in the regulation of fatty acid oxidation and

lipid metabolism^[7]. In the rodents's retinas, the ganglion cell layer (GCL), inner nuclear layer (INL), outer nuclear layer (ONL) and retinal pigment epithelium (RPE) were found to express PPAR α ^[8]. PPAR α expression was down-regulated in diabetic retinas, and the absence of PPAR α aggravated microvascular damage and inflammatory factor upregulation^[8]. Our previous studies revealed that role of fenofibrate (as a PPAR α agonist) in anti-inflammation and anti-oxidant in the HFD-induced retina^[9-10]. However, it was unclear whether the advantages of fenofibrate depended on PPAR α . In this study, we used *PPAR α* knockout mice to study the action of PPAR α -mediated lipid metabolism in the pathological changes and dysfunction in HFD-induced mice retina, as well as the underlying mechanisms.

MATERIALS AND METHODS

Ethical Approval Suzhou Institute of Biomedical Engineering and Technology, Chinese Academy of Sciences approved this investigation by ethical guidelines (approval number: 2019-B20). Animals were used, following the guidelines of the Association for Research in Vision and Ophthalmology (ARVO).

Animal Model On a C57BL/6J background, we used male wild-type C57BL/6J mice and *PPAR α* -knockout mice.

PPAR α ^{-/-} mice came from Jackson Laboratory (USA), while C57BL/6J mice came from Shanghai Slack Laboratory Animal Center. With temperatures range of 22°C to 25°C, animals were housed in a controlled environment with humidity between 55% and 60%. The subjects were maintained in a standard pathogen-free setting with alternate 12-hour light and dark periods. Both C57BL/6J and *PPAR α* ^{-/-} mice were assigned to either a standard-fat diet (SD, 10 kcal% fat, Cat#D12450J, Jiangsu XIETONG Bioengineering Co., Ltd, China) or an HFD (60 kcal% fat, Cat#D12492, Jiangsu XIETONG Bioengineering Co., Ltd, China) at 4 weeks old. Following the 4mo of the respective diet, electroretinography (ERG) was performed. Subsequently, mice were euthanized by inhalation of anesthetics and then used for tissue studies.

Triglyceride Assay The Abcam (ab65336) triglyceride assay kit was used to measure the retinal triglyceride content. Neuroretina (without RPE) tissues were rinsed with chilled phosphate buffer saline (PBS) and weighted from single one eye per mouse. Each sample (1 mg) was resuspended and homogenized with 100 μ L 5% NP-40/ddH₂O solution. The mixture was heated (80°C–100°C) until opaque, cooled to room temperature, and centrifuged to remove insoluble materials. Triglycerides were measured using a fluorometric microplate reader at 535/587 nm (Ex/Em).

Malondialdehyde Detection Assay Malondialdehyde (MDA) detection kit, obtained from Beyotime, was used to measure the level of MDA in the neuro-retina. The neuro-retina tissue was

swiftly rinsed with chilled PBS and subsequently immersed in cold RIPA lysis buffer. Tissue lysate was combined with the kit contents in accordance with the guidance of manufacturer. At 532 nm, absorbance was determined after 15min of incubation at 100°C.

Western Blot Analysis Isolated neuro-retina were extracted in cold RIPA lysis buffer (Beyotime, Nantong, China) composed of a protease and phosphatase inhibitor cocktail (Beyotime, Nantong, China). Protein concentration was measured by BCA protein assay kit in accordance with the manufacturer's instructions (P0012, Beyotime, Nantong, China). Equal amounts of protein samples (30 μ g) were subjected to electrophoresis on 10% or 15% tris-glycine sodium dodecyl sulfate (SDS) polyacrylamide gel and then transferred to a polyvinylidene fluoride (PVDF) membrane. After blocking in 5% bovine serum albumin (BSA) at room temperature (RT) for 1h, the membranes were incubated overnight at 4°C with primary antibodies. After washing three times (5min per time) with tris-buffered saline containing 0.1% Tween-20 (TBST), the membranes were incubated for 1h at RT with secondary antibodies for HRP-conjugated goat anti-rabbit immunoglobulin G (IgG) or goat anti-mouse IgG. The protein bands were developed by enhanced chemiluminescence method and detected using a commercial imaging system (ChemiScope 6300; Clinx Science Instrument Co. Ltd, Shanghai, China).

Quantitative Reverse Transcription Polymerase Chain Reaction Total RNA of the neuro-retina was extracted using RNA Extraction Kit (Beyotime, Nantong, China). The reverse transcription kit (Hifair[®] II 1st Strand cDNA Synthesis SuperMix, YEASEN, Shanghai, China) was used to reverse transcribe it into cDNA. Real-time polymerase chain reaction (PCR) was performed with a Thermo Real-Time PCR detection system (Thermo Fisher Scientific, Massachusetts, USA) using the Hieff Unicon[®] Universal TaqMan multiplex quantitative polymerase chain reaction (qPCR) master mix (YEASEN, Shanghai, China). The amplification program included an initial denaturation step at 95°C for 5min, followed by 45 cycles of 95°C for 15s and 60°C for 30s according to manufacturer. Subsequently, a melt curve analysis was performed to access amplification specificity. The specific gene products were amplified using the primer pairs. Differential gene expression was calculated according to the comparative threshold cycle (CT) method and normalized to β -actin expression as an internal control. The 2^{- $\Delta\Delta$ CT} method was used to quantify mRNA expression.

Immunofluorescence Staining After being removed from the animals, mice eyes were fixed in a 4-degree 4% paraformaldehyde solution for an hour. Eye cups were incubated in sucrose gradients (10% to 30%) and embedded

in OCT compound after removing the cornea and lens. Retina cryosections were obtained with a 12 μm thickness. After washing in PBS, the frozen sections were incubated in 0.3% Triton X-100 for 20min. Following this, they were blocked with 5% BSA for 1h and then covered with primary antibodies at 4°C overnight. The secondary antibodies Alexa Fluor 488-conjugated IgG was applied for 1h in the dark environment at RT. 4,6-Diamino-2-phenyl indole (DAPI) was used for nuclear staining, and a Leica TCS SP5 confocal microscope (Leica Microsystems, Germany) was used to capture images. Image J software was used to determine the immunofluorescence intensity.

Hematoxylin-Eosin Staining The enucleated mice eyes were fixed in FAS eyeball fixative (G1109, Servicebio, Wuhan, China) for 24h at 4°C. Next, they were embedded in paraffin, cut into 5- μm -thick sagittal sections and then stored at RT. Hematoxylin-eosin (H&E) staining of retina were performed after the sections were deparaffinized and rehydrated. The images were observed and imaged with a light microscope (Eclipse E100, Nikon Instruments, Melville, NY, USA).

Electroretinography A Diagnosys system (USA) was used to record ERG recordings. Isoflurane was used to anesthetize animals after over dark-adapted. Pupils were dilated with tropicamide/phenylephrine hydrochloride under dim red light. Under scotopic problems, mice were exposed to full-field pale light intensities of 0.01, 0.01, and 1.01 cd/m^2 . From the baseline to the initial trough, the a-wave amplitude was determined. Between the heights of an a-wave and b-wave, the b-wave amplitude was measured. On a 40 cd/m^2 green background, photopic negative response (PhNR) wave was recorded at a stimulus intensity of 20 cd/m^2 . From the b-wave peak to the PhNR trough, the PhNR wave amplitudes were calculated.

Statistical Analysis For the analysis of statistical data, GraphPad Prism 5.01 (GraphPad Software, USA) was utilized. Mean \pm standard error of the mean (SEM) was used to represent all results. One-way or two-way ANOVA was used to determine statistical significance between groups with Tukey's post-hoc check. *P* values lower than 0.05 were determined to be statistically significant.

RESULTS

PPAR α Deficiency Exacerbated Obesity and Retinal Lipid Metabolic Abnormality Induced by HFD Compared to those on a SD, C57BL/6J mice gained significantly more weight after 4mo of HFD (Figure 1A). Comparing to HFD-fed C57BL/6J mice for 4mo, their body weight increased markedly in HFD-fed PPAR α ^{-/-} mice (Figure 1A). Furthermore, after 4mo on the HFD, the levels of retinal triglyceride were significantly higher than those of age-matched C57BL/6J mice (SD 4M _C57BL/6J: about 0.9957 mg/g, HFD 4M _

C57BL/6J: about 1.954 mg/g; Figure 1B). A much higher level of total triglycerides was detected in the retina of PPAR α ^{-/-} mice (HFD 4M _ PPAR α ^{-/-}: about 3.644 mg/g) compared with that of C57BL/6J mice after 4mo on the HFD (Figure 1B). This indicated that HFD-induced triglyceride accumulation in retina was worsened by PPAR α deficiency.

Increased levels of natural ligand free fatty acid (FFA) can increase PPAR α ability to function as ligand-activated transcription factor. The rate-limiting enzyme in the FFA-oxidation process is regarded as carnitine palmitoyl transferase 1 alpha (CPT1 α) mediating translocation of FFA. In addition, CPT1 α acts a downstream of PPAR α , which provides one evidence of PPAR α activation for the reason that this transcription factor stimulates CPT1 α upregulation. However, rare study investigated the changes of PPAR α and CPT1 α expression in HFD-fed mice retina. Therefore, we determined the protein levels of PPAR α and CPT1 α in the HFD-induced retina using Western blot. Their expression levels significantly rose after 4mo of HFD management compared to the C57BL/6J mice (Figure 1C–1E). However, PPAR α deficiency did not demonstrate an upregulation of CPT1 α expression induced by 4mo of HFD feeding (Figure 1C–1E). Immunofluorescence staining showed that HFD for 4mo increased CPT1 α expression level in the inner retina (mainly in the GCL layer) of C57BL/6J mice, however, PPAR α deficiency did not show an upregulation of CPT1 α expression induced by HFD (Figure 1F, 1G).

HFD-Induced Inflammation in Retina Exacerbated by PPAR α Deficiency Primitive macrophage in the yolk sac is the source of microglia which is the central nervous system's (CNS) resident macrophages^[11]. Upon CNS injury, they migrate to sites of damage and polarize to an activated state ("amoeboid change" in shape) and produce pro-inflammatory cytokines^[11]. In the retina of HFD-fed C57BL/6J mice, there was an increase in the number of Iba-1⁺ microglia and an "amoeboid modification" in the shape of Iba-1⁺ microglia (Figure 2A, 2B). Compared to HFD-induced C57BL/6J mice, the number of Iba-1 positive cells considerably increased in the retina of HFD-induced PPAR α ^{-/-} mice (Figure 2A, 2B). Moreover, "amoeboid change" Iba-1⁺ cells (synapses section) migrated to the ONL (Figure 2A). The results indicated that PPAR α deficiency exacerbated the activation and migration of microglia from the inner to the outer retina after 4mo of receiving HFD. Immunofluorescence staining showed that the quantification of tumor necrosis factor- α (TNF α) fluorescence intensity was increased in the HFD-fed C57BL/6J mice compared with SD-fed C57BL/6J mice. Besides, PPAR α gene knockout significantly increased TNF α levels in most retinal layers (mainly in the GCL layer) after 4mo of HFD administration (Figure 2C, 2D).

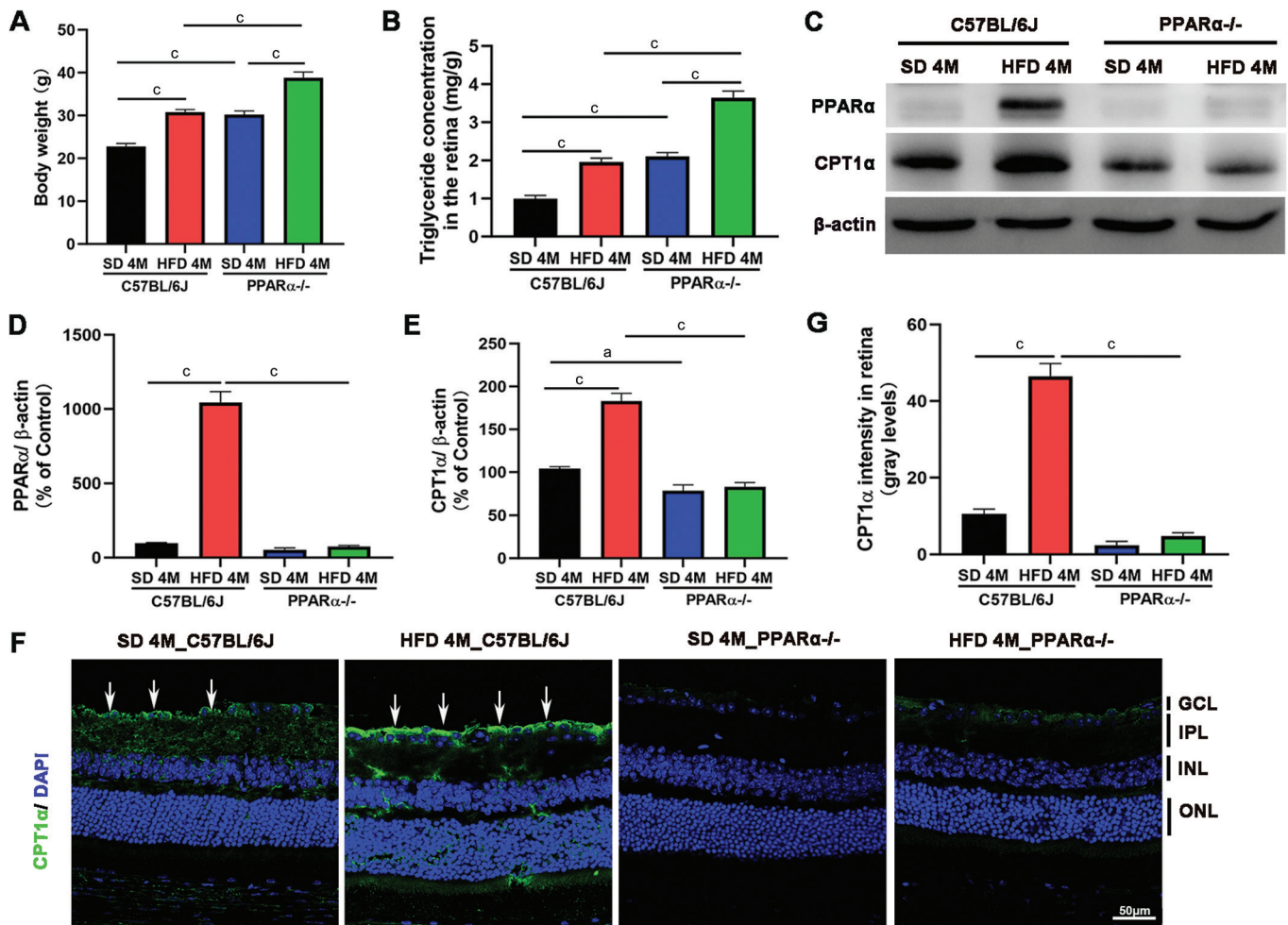


Figure 1 Obesity and abnormal retinal lipid metabolism brought on by HFD were increased by *PPAR α* knockout For a duration of 4mo, C57BL/6J and *PPAR α ^{-/-}* mice were given either a SD or HFD. A: Body weight was examined for mice; B: Triglyceride assay showed the content of triglyceride in retina; C: Representative Western blot images of the retina's *PPAR α* and *CPT1 α* proteins; D, E: Statistical analysis of Western blot. F: Representative immunofluorescence images of *CPT1 α* in the retina (blue: DAPI; green: *CPT1 α*). Arrows indicated *CPT1 α* positive staining. G: *CPT1 α* fluorescent intensity measurement using Image J software (scale bar: 50 μ m). *n* is 5 per group. ^a*P*<0.05, ^c*P*<0.001. HFD: High-fat diet; *PPAR α* : Peroxisome proliferator activated receptor-alpha; SD: Standard diet; *CPT1 α* : Carnitine palmitoyl transferase 1 alpha; DAPI: 4,6-Diamino-2-phenyl indole; GCL: Ganglion cell layer; IPL: Inner plexiform layer; INL: Inner nuclear layer; ONL: Outer nuclear layer.

Nuclear factor-kappa B (NF- κ B) signaling pathway is crucial in modulating innate immune and inflammatory responses. Typically, inflammatory cytokines production, such as TNF α , interlenkin (IL)1 β and IL6, is usually promoted by the activated NF- κ B signaling pathway. We examined the ratio of p-NF- κ B p65 to NF- κ B p65 and corresponding proinflammatory cytokine levels to further assess the role of *PPAR α* deficiency in HFD-induced inflammation in retina. Compared to SD-fed C57BL/6J mice, Western blot results revealed that p-NF- κ B p65/NF- κ B p65 was upregulated in the retina of HFD-fed mice (Figure 2E, 2F). *PPAR α* deficiency induced a much higher level of p-NF- κ B p65/NF- κ B p65 after HFD for 4mo (Figure 2E, 2F). As shown in Figure 2E, 2G–2J, the expression of TNF α , ICAM1, IL1 β and IL6 were markedly up-regulated in HFD-fed C57BL/6J and SD-fed *PPAR α ^{-/-}* mice retina, and were even higher in HFD-induced *PPAR α ^{-/-}* mice

retina. These results demonstrated that HFD-induced activation of the NF- κ B signaling pathway in retina was exacerbated by *PPAR α* gene knockout.

***PPAR α* Deficiency Exacerbated Oxidative Stress Induced by HFD** Free radicals remove electrons from lipids, leading to the formation of reactive intermediates, in the process known as lipid peroxidation^[12]. Traditionally, MDA serves as a widely recognized indicator for assessing lipid peroxidation levels. After 4mo of a HDF, MDA formation levels in the retina were noticeably higher in this study (Figure 3A). *PPAR α* deficiency exacerbated MDA accumulation compared with WT mice induced by an HFD for 4mo (Figure 3A). 4-HNE, a pivotal mediator of oxidative stress, can be produced as a hazardous product from lipid peroxides. In the RPE tissue, 4-HNE has been used to cause oxidative stress and as an important indicator of lipid peroxidation/oxidative stress^[13-14]. Western

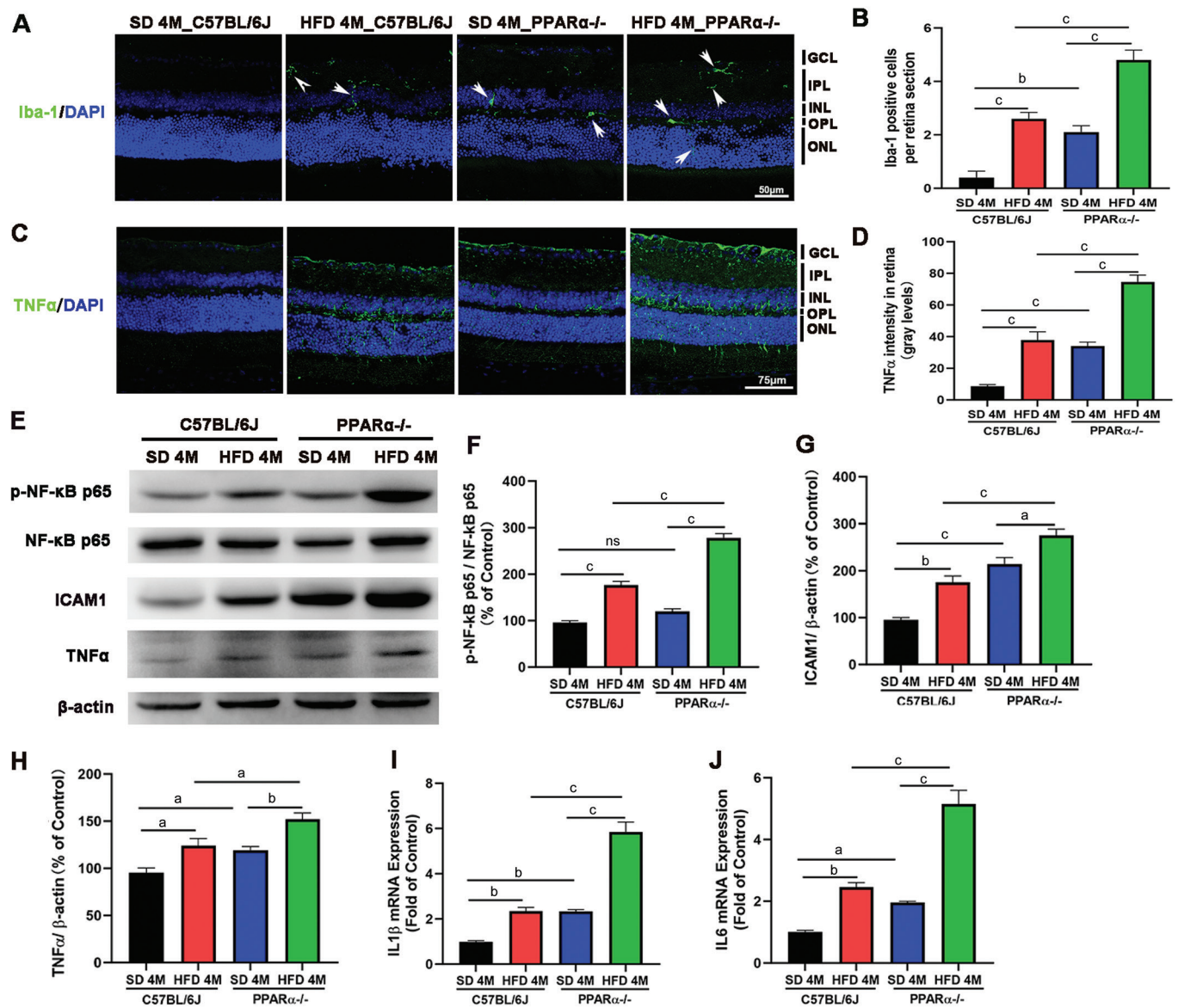


Figure 2 PPAR α deficiency accelerated HFD-induced inflammatory cell infiltration and NF- κ B signaling activation in the retina. Male C57BL/6J and PPAR α ^{-/-} mice were assigned to either a SD or HFD for a duration of 4mo. A: Representative immunofluorescence images of Iba-1⁺ microglia (blue: DAPI; green: Iba-1) in the retina. Arrows indicated positively stained microglia. B: The retinal Iba-1 positive cell was quantified; C: Representative immunofluorescence images of TNF α (blue: DAPI; green: TNF α) in the retina; D: Quantification of TNF α fluorescent intensity in the retina; E: Representative Western blot images showing the protein levels of p-NF- κ B p65, NF- κ B p65, ICAM1, TNF α , and β -actin in the retina; F: Quantitative analysis of the p-NF- κ B p65/NF- κ B p65 ratio; G, H: Quantification of ICAM1 and TNF α protein levels based on Western blot results; I, J: Real-time PCR results exhibited proinflammatory factors IL1 β (I) and IL6 (J) mRNA expression levels in the retina. Scale bar: 50 μ m (A). Scale bar: 75 μ m (C). *n* is 5 per group. ns: No significance. ^a*P*<0.05, ^b*P*<0.01, ^c*P*<0.001. NF- κ B: Nuclear factor-kappa B; HFD: High-fat diet; PPAR α : Peroxisome proliferator activated receptor-alpha; SD: Standard diet; DAPI: 4,6-Diamino-2-phenyl indole; TNF α : Tumor necrosis factor- α ; p-NF- κ B: Phosphorylated nuclear factor-kappa B; ICAM1: Intercellular adhesion molecule-1; PCR: Polymerase chain reaction; IL: interlenkin; GCL: Ganglion cell layer; INL: Inner nuclear layer; IPL: Inner plexiform layer; OPL: Outer plexiform layer; ONL: Outer nuclear layer.

blot analysis demonstrated that a four-month HFD resulted in a notable elevation in the amounts of 4-HNE relative to that in the C57BL/6J mice fed with SD (Figure 3B, 3C). Furthermore, 3-NT has emerged as a significant indicator of oxidative stress, which arises from the nitration of protein associated with free tyrosine residues^[15]. Similar results were obtained from Western blot analysis, which revealed a 3-NT level

increased after 4mo on the HFD (Figure 3B, 3D). Compared to C57BL/6J mice with 4mo of HFD, Western blot analysis revealed elevated protein expressions of 3-NT and 4-HNE in the retina of HFD-fed PPAR α knockout mice (Figure 3B–3D). After 4-month of HFD, Immunofluorescence staining showed a significant increase in 3-NT staining in GCL of C57BL/6J mice (Figure 3E).

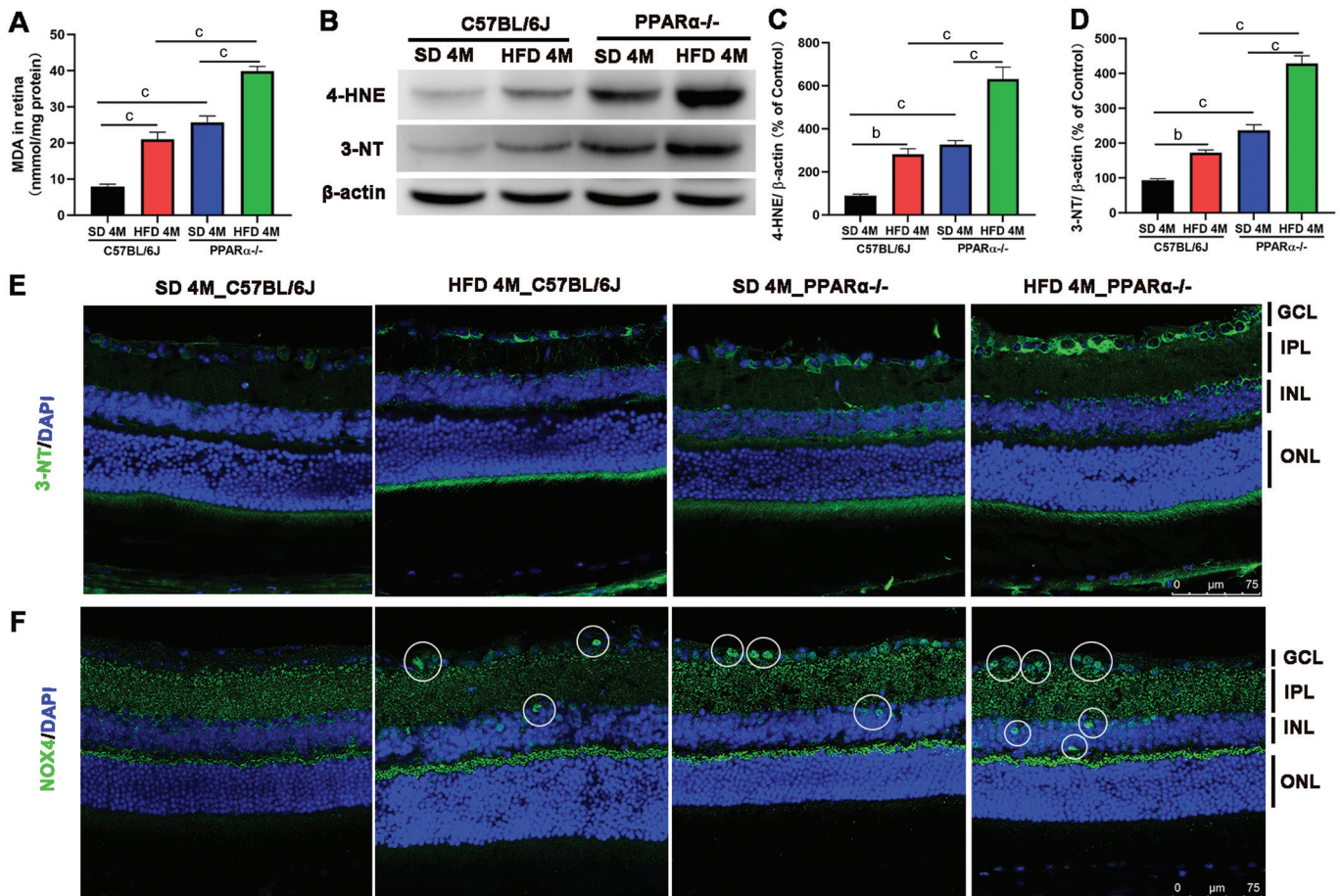


Figure 3 PPARα deficiency accelerated oxidative stress induced by HFD For 4mo, mice from the C57BL/6J and PPARα^{-/-} were either exposed to a SD or HFD. A: MDA levels in the retina were measured using an MDA detection kit. B–D: Representative Western blot images (B) and corresponding statistical analyses (C, D) showing protein levels of 4-HNE (B, C) and 3-NT (B, D) in the retina. E, F: Representative immunofluorescence images showing 3-NT (green: 3-NT; blue: DAPI) and NOX4 (green: NOX4; blue: DAPI) expression from the GCL to INL layers (scale bar: 75 μm). The white circle indicated positive staining. *n*=5/group. ^b*P*<0.01, ^c*P*<0.001. MDA: Malondialdehyde; 4-HNE: 4-Hydroxynonenal; NOX4: Nicotinamide adenine dinucleotide phosphate oxidase 4; HFD: High-fat diet; PPARα: Peroxisome proliferator activated receptor-α; SD: Standard diet; DAPI: 4,6-Diamino-2-phenyl indole; GCL: Ganglion cell layer; INL: Inner nuclear layer; IPL: Inner plexiform layer; ONL: Outer nuclear layer.

PPARα deficiency and HFD induced a much higher expression level of 3-NT not only in GCL but also in INL (Figure 3E). We observed that HFD or PPARα deficiency increased the NOX4 staining from the GCL to INL layers (Figure 3F). PPARα^{-/-} mice showed a higher level of NOX4 staining from the GCL to INL layers following 4mo of HFD (Figure 3F). Collectively, these findings indicated that PPARα gene knockout contributed to the increase in oxidative stress triggered by HFD in the retina, particularly in the inner layer of the retina.

PPARα Deficiency Exacerbated HFD-Induced Apoptosis Initiation in Retina Previous studies reported that both oxidative stress^[16] and inflammation^[17] were the important reasons triggering an apoptotic response. Caspase3 and poly ADP-ribose polymerase (PARP) were proteolytically cleaved and in turn activated at the onset of apoptosis. Therefore, the expression levels of the apoptosis regulator cleaved-Caspase-3 and cleaved-PARP were consequently evaluated. The HFD for

4mo led to enhanced cleavage of PARP and Caspase-3 in the C57BL/6J mice retina, and resulted in even higher levels in the PPARα^{-/-} mice retina (Figure 4A–4C). Immunofluorescence staining showed that PPARα gene knockout significantly increased cleaved-Caspase3 levels in the GCL layer after 4mo of HFD administration (Figure 4D). H&E staining was used to assess the morphology of neural retina. We found that there were no effects of HFD for 4mo or (and) PPARα deficiency on the morphology of neural retina (Figure 4E). Taken together, PPARα deficiency distinctly induced RGC cell apoptosis initiation but no obvious histological change in the retina after the HFD induction for 4mo.

HFD-Induced Retinal Dysfunction Exacerbated by PPARα Deficiency Full-field ERG was performed under both scotopic and photopic problems to further evaluate whether HFD and PPARα deletion could lead to retinal dysfunction. The photoreceptors and bipolar cells functions, respectively,

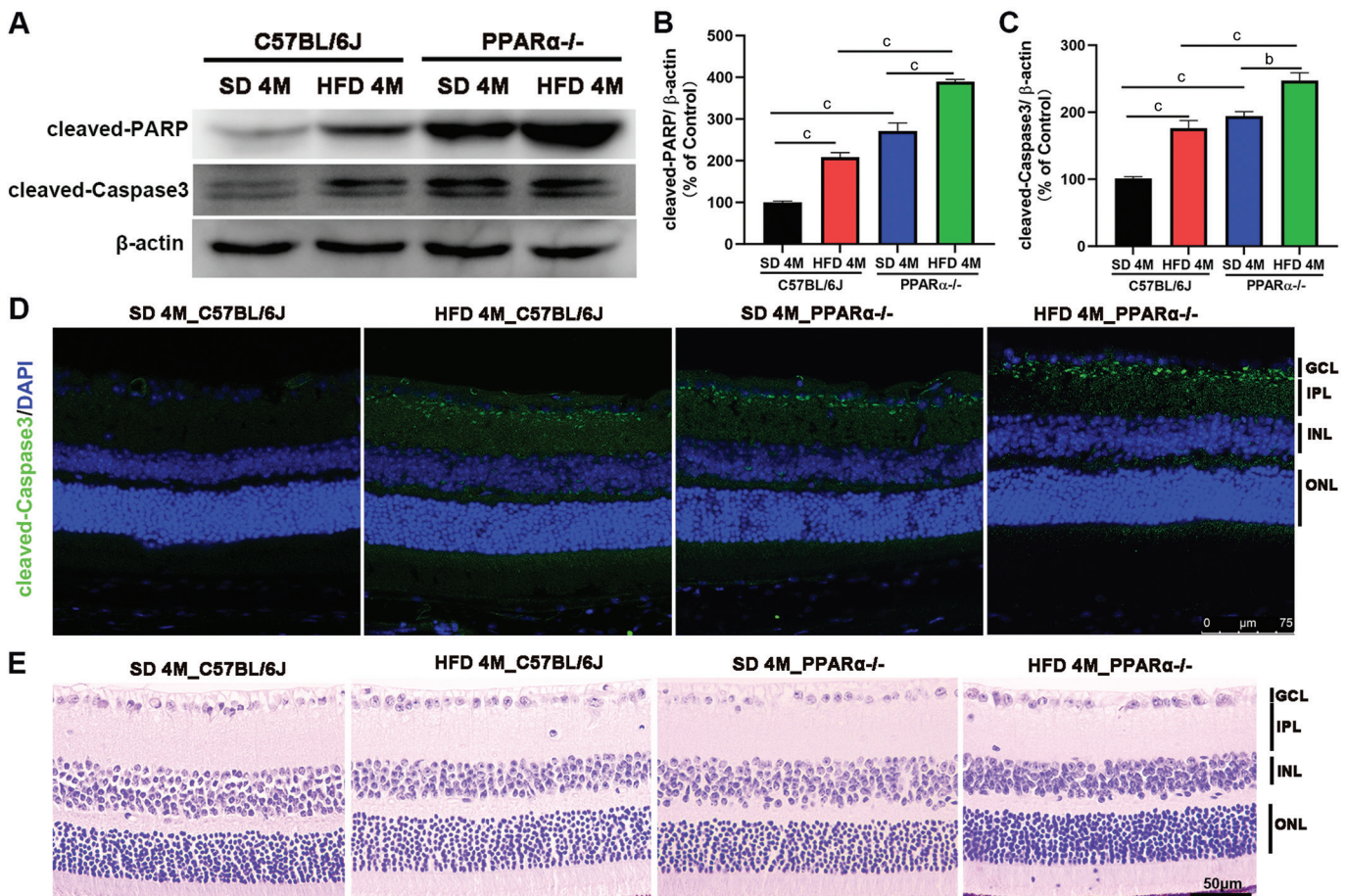


Figure 4 PPAR α deficiency accelerated HFD-induced apoptosis in the retina For a duration of 4mo, C57BL/6J and PPAR α ^{-/-} mice were exposed to either a SD or HFD. A–C: Representative Western blot images (A) and statistical analysis (B, C) showing the expression levels of apoptosis regulator cleaved-PARP (A, B) and cleaved-Caspase3 (A, C) protein levels in retina. D: Immunofluorescence staining of cleaved-Caspase3 (in the cytoplasmic) in the retina (scale bar: 75 μ m; green: cleaved-Caspase3, blue: DAPI). E: Hematoxylin-eosin staining of the retina (scale bar: 50 μ m). $n=5$ /group. ^b $P<0.01$, ^c $P<0.001$. PARP: Poly ADP-ribose polymerase; HFD: High-fat diet; PPAR α : Peroxisome proliferator activated receptor- α ; SD: Standard diet; DAPI: 4,6-Diamino-2-phenyl indole; GCL: Ganglion cell layer; INL: Inner nuclear layer; IPL: Inner plexiform layer; ONL: Outer nuclear layer.

were indicated by the a- and b-wave amplitudes. HFD for 4mo significantly reduced a-wave amplitudes under scotopic conditions (1.0 cd·s/m² stimulus luminance; Figure 5A, 5C). Moreover, the scotopic a-wave amplitude of PPAR α ^{-/-} mice was much lower after 4mo of HFD administration (1.0 cd·s/m² stimulus luminance; Figure 5A, 5C). Consistently, HFD for 4mo decreased amplitudes of scotopic b-wave in the WT mice (0.1 cd·s/m² and 1.0 cd·s/m² stimulus luminance), especially in the PPAR α knockout mice (Figure 5A, 5D). In addition, PhNR wave was performed to evaluate the function of RGCs. We found that HFD for 4mo significantly decreased the amplitudes of PhNR-wave in the C57BL/6J mice, and resulted in the even lower amplitude in PPAR α ^{-/-} mice (Figure 5B, 5E). These results indicated that HFD feeding induced retinal dysfunction in C57BL/6J mice, and even more so in PPAR α ^{-/-} mice.

DISCUSSION

Animal models subjected to HFD have commonly been utilized in research related to diabetes, metabolic syndrome and obesity.

Recently, the effects of HFD on the retinal degeneration has become a popular topic^[6,18-19]. However, the direct role of lipid metabolism in HFD-induced retinal degeneration remained unclear. Our data demonstrated that excessive fatty acid consumption increased triglycerides accumulation in retina. As a major source of fuel, triglycerides can be hydrolyzed into FFA. PPAR α can be activated by increased concentration of natural ligand FFA, which in turn increased energy combustion and alleviated excessive accumulation of lipid by regulating β -oxidation of FFA (FAO)^[20]. There was a notable reduction in PPAR α levels within the retinas of diabetic rats induced by streptozotocin (STZ), Akita mice and *db/db* mice^[8]. Inconsistently, our results showed that significant upregulations of PPAR α and its downstream CPT1 α level in C57BL/6J mice fed with HFD. The complex network of lipid and glucose metabolism might contribute to the regulation of PPAR α expression under different conditions.

Besides, PPAR α ^{-/-} mice fed with HFD didn't show the

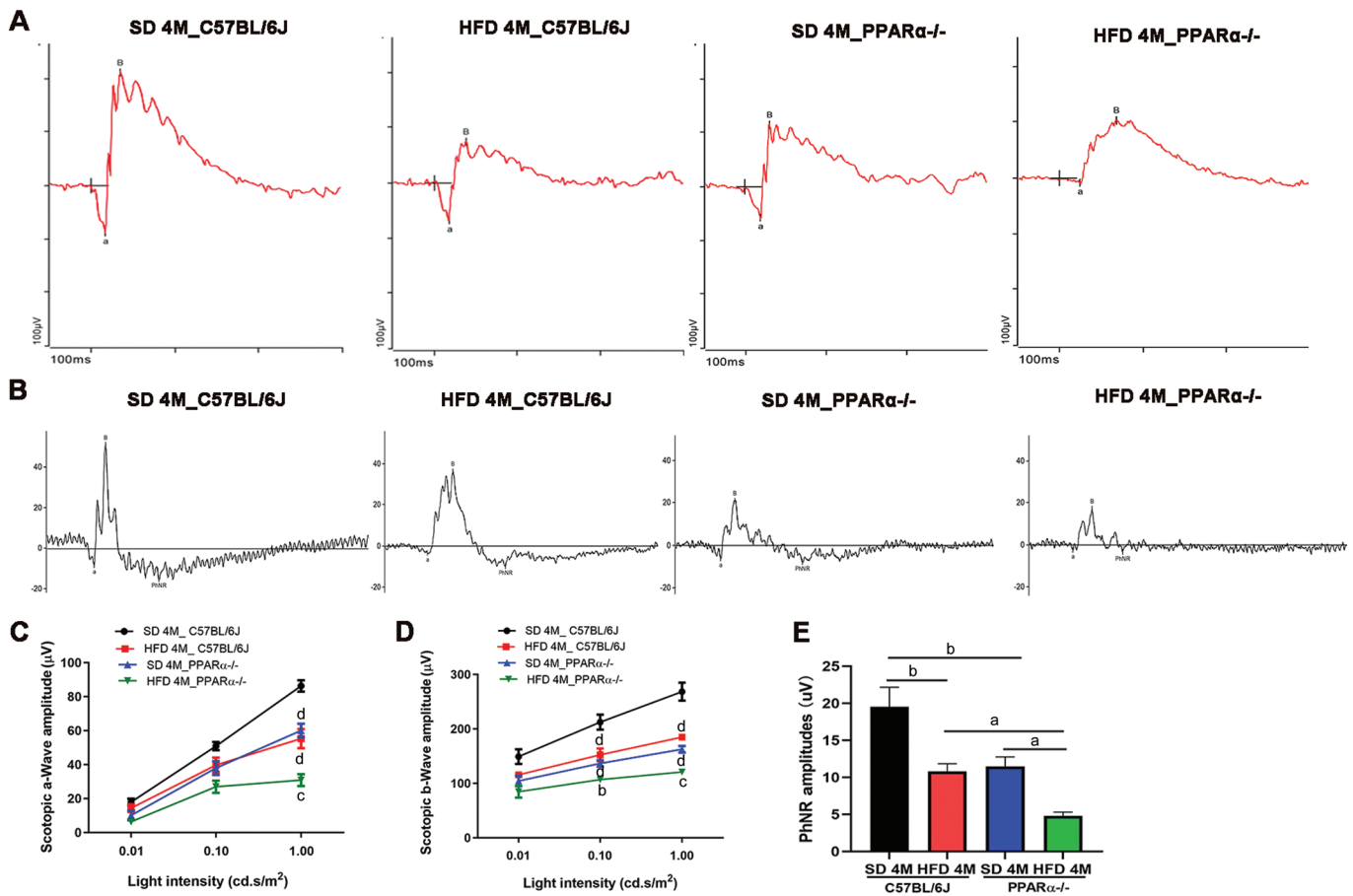


Figure 5 PPAR α deficiency exacerbated HFD-induced retinal dysfunction C57BL/6J and PPAR α ^{-/-} mice were subjected to either a SD or HFD for a duration of 4mo. A: Representative electroretinogram plots for the four experimental groups at a stimulus intensity of 1.0 cd·s/m² under scotopic conditions; B: Representative PhNR waves for four groups at 20 cd·s/m² on a green background of 40 cd·s/m²; C, D: Statistical analysis of amplitude changes of a-wave (C) and b-wave (D) at different stimulus intensities (0.01, 0.1, 1.0 cd·s/m²) under scotopic conditions. *n*=7/group. ^b*P*<0.01 vs HFD 4M_C57BL/6J; ^c*P*<0.001 vs HFD 4M_C57BL/6J; ^d*P*<0.001 vs SD 4M_C57BL/6J. Bar graphs represent mean values±SEM. E: Statistical analysis of amplitude changes of PhNR waves. *n*=10-12/group. E: ^a*P*<0.05, ^b*P*<0.01. HFD: High-fat diet; PPAR α : Peroxisome proliferator activated receptor- α ; SD: Standard diet; SEM: Standard error of the mean; PhNR: Photopic negative response.

upregulations of PPAR α and CPT1 α protein expression in the retina. Based on the above, we speculated that HFD for 4mo induced a self-protection behavior by upregulating PPAR α and CPT1 α expression against lipid accumulation. However, PPAR α ^{-/-} retina was defective in β -oxidation and showed loss of compensatory ability to counteract lipid accumulation induced by HFD. Consistent with above hypothesis, the higher triglycerides contents were found in the retina of PPAR α ^{-/-} mice compared to C57BL/6J mice after 4mo of HFD. We further found that CPT1 α mainly located in the inner retinal, especially in the GCL layer. Collectively, we further speculated that PPAR α ablation increased HFD-induced abnormal lipid accumulation via the induction of abnormal lipid metabolism in the inner retinal (especially GCL cells).

Lipids used as oxidizable substrates might yield more ATP than glucose in the process of signal transduction of retinal neurons^[21]. However, HFD associated with excessive lipid accumulation increased the number of CD11b⁺ or CD45⁺

macrophages or microglia in the inner retina, from the OPL to the RGC^[22]. This was considered to be the response of retinal microglia to lipid metabolic disorder. Furthermore, activated microglia could evolve into inflammatory effector cells releasing inflammatory cytokines. Our prior study showed that HFD for 5mo increased the Iba-1⁺ microglia infiltration in the inner retina, accompanied with NF- κ B and JNK pathway activation^[9]. Consistently, this study also showed that HFD for 4mo induced Iba-1⁺ microglia cells infiltration in the inner retina, accompanied with an activation of the NF- κ B signaling pathway. On the other hand, recent study demonstrated that PPAR α knockout significantly up-regulated inflammatory regulators in CD11b⁺ cells located in the inner retina^[23]. More importantly, our previous study demonstrated that fenofibrate, as the PPAR α agonist, inhibited the microglia infiltration, and in turn alleviated retinal inflammation after 5mo on the HFD in a mouse model^[9]. However, another study showed that fenofibrate prevented the development of type

II diabetic retinopathy without upregulation of PPAR α in the retina^[24]. Therefore, it was not known whether fenofibrate's anti-inflammatory action depended on PPAR α in HFD-induced retina. In the present study, we found that PPAR α deficiency exacerbated HFD-induced microglia infiltration and activation from inner retina to outer retina. Consistently, PPAR α deficiency aggravated retinal dysfunction, including photoreceptor cells, bipolar cells and ganglion cells. Therefore, we speculated that the lack of PPAR α exacerbated microglia overactivation response to lipid accumulation, which in turn increased HFD-induced retinal inflammation.

As the above noted, microglia activation might be associated with lipid accumulation. Other studies found that reactive oxidative species production could stem from an overactivation of either macrophages or microglia in the CNS and retina^[22]. Interestingly, intracellular lipid accumulation could induce oxidative stress based on the increased levels of reactive oxygen species levels and lipid peroxidation^[25]. In this study, HFD increased the expression of oxidative stress in the inner retina and lipid peroxidation in the retina. Further, PPAR α deficiency further increased HFD-induced the upregulations of oxidative stress marker 3-NT in the inner retina, as well as indicators of lipid peroxidation such as 4-HNE and MDA in the retina. Therefore, the possibility existed that PPAR α knockout exacerbated HFD-induced oxidative stress in the inner retina directly or indirectly through lipid accumulation. These findings highlighted the contribution of lipid metabolism disorders associated with PPAR α to inflammation and oxidative stress in the retina. Inflammation and oxidative stress are closely interconnected processes, particularly in metabolic disorders such as those induced by HFD. Previous studies suggested that the potential feedback loop between inflammation and oxidative stress processes^[26-27]. Further, more studies are needed to investigate the causative relationship between inflammation and oxidative stress based on the lipid metabolism disorders.

PPAR α has a potent protective role in the retinal vascular disease, such as ischemic and diabetic retinopathy^[28-29]. However, the role of PPAR α in RGC cells has relatively little attention to date. Our data demonstrated that PPAR α knockout increased the HFD-induced RGC cells apoptosis initiation which was consistent with CPT1 α (as the downstream of PPAR α) location, as well as lipid accumulation, enhanced inflammation and oxidative stress in the retina. Oxidative stress associated with lipid peroxidation serves as a crucial factor in the advancement of neurodegeneration^[30-32]. Furthermore, the increase in inflammation agents directly acted on RGC to induce cell death^[18]. Therefore, we proved the hypothesis: the lack of PPAR α might initially induce lipid metabolism disorder, in turn exacerbate inflammation and oxidative stress,

and eventually aggravate RGCs apoptosis initiation and dysfunction. In addition, another possibility also deserved more attention regarding the crosstalk between triglyceride accumulation and glucose metabolic abnormalities. Previous studies have shown that HFD aggravated glucose metabolism disorders^[33]. Therefore, excess lipid accumulation in the retina contribution to disruptions in glucose metabolism, potentially played an essential role in HFD-induced retinal degeneration, particularly in the context of PPAR α deficiency.

In summary, our study indicated that PPAR α deficiency exacerbated lipid metabolic abnormalities, inflammatory responses, oxidative stress, apoptosis initiation and dysfunction in HFD-fed mice retina, especially in the inner retina. This research sheds light on how disorders in lipid metabolism could induce negative changes in the retina and potentially trigger the development of a retinopathy. Besides, PPAR α ^{-/-} mice may be used as a model to help us to study the relationship between lipid metabolism and retinal dysfunction. More importantly, this study indicated that the potential role of PPAR α activation in treating RGC injury (such as glaucoma, retinal ischemia-reperfusion damage). Nevertheless, it proved challenging to delineate the exact effects of PPAR α and lipid metabolism on a separate cell layer, as well as the interactions between neuronal and microglia cells, because the pathological changes involve various cell types and intricate interactions within the retina. Further research is necessary to address these questions.

ACKNOWLEDGEMENTS

Authors' Contributions: Wang X and Jiang ZX designed the experiments. Wang X, Ding JJ, Yu CF, and Xiao DC conducted the experiments and analyzed the experimental data. Wang X drafted the manuscript. Jiang ZX and Tao LM revised the manuscript. All authors approved the final version of manuscript.

Foundations: Supported by the Anhui Medical University Research Fund (No.2023xkj035); National Natural Science Foundation Incubation Program Project of the Second Affiliated Hospital of Anhui Medical University (No.2023GQFY05); the Key Research and Development Technology project of Anhui Province (No.2022j11020013).

Conflicts of Interest: Wang X, None; Ding JJ, None; Yu CF, None; Xiao DC, None; Tao LM, None; Jiang ZX, None.

REFERENCES

- 1 Zhu HZ, Zhang WZ, Zhao YY, *et al.* GSK3 β -mediated tau hyperphosphorylation triggers diabetic retinal neurodegeneration by disrupting synaptic and mitochondrial functions. *Mol Neurodegener* 2018;13(1):62.
- 2 Vidal E, Lalarme E, Maire MA, *et al.* Early impairments in the retina of rats fed with high fructose/high fat diet are associated with glucose metabolism deregulation but not dyslipidaemia. *Sci Rep* 2019;9(1):5997.

- 3 Asare-Bediako B, Noothi SK, Li Calzi S, *et al.* Characterizing the retinal phenotype in the high-fat diet and western diet mouse models of prediabetes. *Cells* 2020;9(2):E464.
- 4 Wang M, Lv JY, Huang XS, *et al.* High-fat diet-induced atherosclerosis promotes neurodegeneration in the triple transgenic (3 × Tg) mouse model of Alzheimer’s disease associated with chronic platelet activation. *Alzheimers Res Ther* 2021;13(1):144.
- 5 Crispino M, Trinchese G, Penna E, *et al.* Interplay between peripheral and central inflammation in obesity-promoted disorders: the impact on synaptic mitochondrial functions. *Int J Mol Sci* 2020;21(17):E5964.
- 6 Kutsyr O, Noailles A, Martínez-Gil N, *et al.* Short-term high-fat feeding exacerbates degeneration in retinitis pigmentosa by promoting retinal oxidative stress and inflammation. *Proc Natl Acad Sci U S A* 2021;118(43):e2100566118.
- 7 Hu P, Li KQ, Peng XX, *et al.* Nuclear receptor PPAR α as a therapeutic target in diseases associated with lipid metabolism disorders. *Nutrients* 2023;15(22):4772.
- 8 Hu Y, Chen Y, Ding LX, *et al.* Pathogenic role of diabetes-induced PPAR- α down-regulation in microvascular dysfunction. *Proc Natl Acad Sci U S A* 2013;110(38):15401-15406.
- 9 Wang X, Yu CF, Liu XM, *et al.* Fenofibrate ameliorated systemic and retinal inflammation and modulated gut microbiota in high-fat diet-induced mice. *Front Cell Infect Microbiol* 2022;12:839592.
- 10 Wang X, Liu XM, Tzekov R, *et al.* Fenofibrate ameliorates retinal pigment epithelium injury induced by excessive fat through upregulation of PI3K/AKT signaling. *Drug Des Devel Ther* 2023;17: 3439-3452.
- 11 Prinz M, Masuda T, Wheeler MA, *et al.* Microglia and central nervous system-associated macrophages—from origin to disease modulation. *Annu Rev Immunol* 2021;39:251-277.
- 12 Su LJ, Zhang JH, Gomez H, *et al.* Reactive oxygen species-induced lipid peroxidation in apoptosis, autophagy, and ferroptosis. *Oxid Med Cell Longev* 2019;2019:5080843.
- 13 Yang HJ, Hu R, Sun H, *et al.* 4-HNE induces proinflammatory cytokines of human retinal pigment epithelial cells by promoting extracellular efflux of HSP70. *Exp Eye Res* 2019;188:107792.
- 14 Lei L, Tzekov R, Tang SB, *et al.* Accumulation and autofluorescence of phagocytized rod outer segment material in macrophages and microglial cells. *Mol Vis* 2012;18:103-113.
- 15 Bandoowala M, Thakkar D, Sengupta P. Advancements in the analytical quantification of nitrooxidative stress biomarker 3-nitrotyrosine in biological matrices. *Crit Rev Anal Chem* 2020;50(3): 265-289.
- 16 Wang S, Irving G, Jiang LL, *et al.* Oxidative stress mediated hippocampal neuron apoptosis participated in carbon disulfide-induced rats cognitive dysfunction. *Neurochem Res* 2017;42(2):583-594.
- 17 Altmann C, Schmidt MHH. The role of microglia in diabetic retinopathy: inflammation, microvasculature defects and neurodegeneration. *Int J Mol Sci* 2018;19(1):110.
- 18 Cao XP, Guo YT, Wang YC, *et al.* Effects of high-fat diet and Apoe deficiency on retinal structure and function in mice. *Sci Rep* 2020;10:18601.
- 19 Roddy GW, Rosa RH, Viker KB, *et al.* Diet mimicking “fast food” causes structural changes to the retina relevant to age-related macular degeneration. *Curr Eye Res* 2020;45(6):726-732.
- 20 Grygiel-Górniak B. Peroxisome proliferator-activated receptors and their ligands: nutritional and clinical implications—a review. *Nutr J* 2014;13:17.
- 21 Pearsall EA, Cheng R, Zhou KL, *et al.* PPAR α is essential for retinal lipid metabolism and neuronal survival. *BMC Biol* 2017;15:113.
- 22 Lee JJ, Wang PW, Yang IH, *et al.* High-fat diet induces toll-like receptor 4-dependent macrophage/microglial cell activation and retinal impairment. *Invest Ophthalmol Vis Sci* 2015;56(5):3041-3050.
- 23 Ma X, Wu WJ, Liang WT, *et al.* Modulation of cGAS-STING signaling by PPAR α in a mouse model of ischemia-induced retinopathy. *Proc Natl Acad Sci U S A* 2022;119(48):e2208934119.
- 24 Enright JM, Zhang S, Thebeau C, *et al.* Fenofibrate reduces the severity of neuroretinopathy in a type 2 model of diabetes without inducing peroxisome proliferator-activated receptor alpha-dependent retinal gene expression. *J Clin Med* 2020;10(1):126.
- 25 Coia H, Ma N, Hou Y, *et al.* Prevention of lipid peroxidation-derived cyclic DNA adduct and mutation in high-fat diet-induced hepatocarcinogenesis by theaaphenon E. *Cancer Prev Res (Phila)* 2018;11(10):665-676.
- 26 Zou M, Ke Q, Nie Q, *et al.* Inhibition of cGAS-STING by JQ1 alleviates oxidative stress-induced retina inflammation and degeneration. *Cell Death Differ* 2022;29:1816-1833.
- 27 Huang CC, Tsai SF, Liu SC, *et al.* Insulin mediates lipopolysaccharide-induced inflammatory responses and oxidative stress in BV2 microglia. *J Inflamm Res* 2024;17:7993-8008.
- 28 Chen Y, Hu Y, Lin MK, *et al.* Therapeutic effects of PPAR α agonists on diabetic retinopathy in type 1 diabetes models. *Diabetes* 2013;62(1):261-272.
- 29 Moran E, Ding LX, Wang ZX, *et al.* Protective and antioxidant effects of PPAR α in the ischemic retina. *Invest Ophthalmol Vis Sci* 2014;55(7):4568-4576.
- 30 Liu L, Zhang K, Sandoval H, *et al.* Glial lipid droplets and ROS induced by mitochondrial defects promote neurodegeneration. *Cell* 2015;160(1-2):177-190.
- 31 Peña-Bautista C, Vento M, Baquero M, *et al.* Lipid peroxidation in neurodegeneration. *Clin Chim Acta* 2019;497:178-188.
- 32 Angelova PR, Esteras N, Abramov AY. Mitochondria and lipid peroxidation in the mechanism of neurodegeneration: Finding ways for prevention. *Med Res Rev* 2021;41(2):770-784.
- 33 Li J, Li X, Zhang Z, *et al.* High-fat diet aggravates the disorder of glucose metabolism caused by chlorpyrifos exposure in experimental rats. *Foods* 2023;12(4):816.